

Effect of intrinsic spin relaxation on the spin-dependent cotunneling transport through quantum dots

Ireneusz Weymann^{1,*} and Józef Barnas^{1,2}

¹*Department of Physics, Adam Mickiewicz University, 61-614 Poznań, Poland*

²*Institute of Molecular Physics, Polish Academy of Sciences, 60-179 Poznań, Poland*

(Dated: May 24, 2019)

Spin-polarized transport through quantum dots is analyzed theoretically in the cotunneling regime. It is shown that the zero-bias anomaly, found recently in the antiparallel configuration, can also exist in the case when one electrode is magnetic while the other one is nonmagnetic. Physical mechanism of the anomaly is also discussed. It is demonstrated that intrinsic spin relaxation in the dot has a significant influence on the zero-bias maximum in the differential conductance – the anomaly becomes enhanced by weak spin-flip scattering in the dot and then disappears in the limit of fast spin relaxation. Apart from this, inverse tunnel magnetoresistance has been found in the limit of fast intrinsic spin relaxation in the dot. The diode-like behavior of transport characteristics in the cotunneling regime has been found in the case of quantum dots asymmetrically coupled to the leads. This behavior may be enhanced by the spin-flip relaxation processes.

PACS numbers: 72.25.Mk, 73.63.Kv, 85.75.-d, 73.23.Hk

I. INTRODUCTION

Electronic transport through nano-scale systems coupled to ferromagnetic leads reveals new phenomena which arise due to the interplay of charge and spin degrees of freedom. In the case of metallic grains or large quantum dots, this leads to magnetic-dependent Coulomb blockade and Coulomb oscillations phenomena^{1,2,3}, spin accumulation, negative differential conductance, and inverse tunnel magnetoresistance (TMR) effect^{4,5,6}. Transport through a quantum dot with a few electrons reveals further features resulting from discreteness of the dot energy spectrum and from electron correlations^{7,8,9,10,11}. When the dot is weakly coupled to the leads, one can distinguish two different regimes of electronic transport: sequential and cotunneling ones^{12,13,14}. Sequential transport through a single-level quantum dot coupled to ferromagnetic leads was studied quite recently for collinear^{15,16} and non-collinear^{17,18,19} configurations of the magnetic moments of electrodes. Spin polarized transport in the cotunneling regime has also been addressed^{20,21,22}. It has been shown²⁰ that the interplay of various spin dependent cotunneling processes gives rise to anomalous behavior of the differential conductance when the leads' magnetic moments are antiparallel. This, in turn, leads to the corresponding zero-bias anomaly in the tunnel magnetoresistance. Moreover, the even-odd electron number parity effect in tunnel magnetoresistance has also been found²³. In both cases intrinsic spin relaxation in the dot was neglected, and spin in the dot could relax only due to cotunneling events.

In this paper we consider transport through single-level quantum dots coupled to ferromagnetic leads in the cotunneling regime. In particular, we show how the intrinsic spin relaxation in the dot affects the dot occupation probabilities, spin accumulation, conductance and the TMR effect. We analyze the cases of quantum dots

with degenerate and non-degenerate energy levels, which are symmetrically (equal spin polarizations of the leads) and asymmetrically (unequal spin polarizations of the leads) coupled to the leads. The latter case is of particular interest as the corresponding transport characteristics are highly asymmetric with respect to the bias reversal. We show that this diode-like behavior may be enhanced by intrinsic spin-flip relaxation processes in the dot. Moreover, we show that the zero-bias anomaly, found previously²⁰ in the antiparallel configuration, can occur in any magnetically asymmetric system, in particular when one electrode is nonmagnetic while the other one is ferromagnetic.

The systems discussed in this paper may be realized experimentally in various ways, including self-assembled dots in ferromagnetic semiconductors²⁴, ultra-small metallic particles²⁵, granular structures²⁶, carbon nanotubes^{27,28,29}, and other molecules³⁰. In the case of quantum dots coupled to nonmagnetic leads, differential conductance in the cotunneling regime has also been measured experimentally³¹.

In section 2 we present the model and theoretical formulation of the problem. Numerical results for symmetric and asymmetric systems are shown and discussed in sections 3 and 4, respectively. Final conclusions are given in section 5.

II. MODEL AND METHOD

We consider a single-level quantum dot coupled to ferromagnetic leads and for simplicity restrict our considerations to the case when magnetic moments of the leads are either parallel or antiparallel. The system is described by the Hamiltonian $H = H_L + H_R + H_D + H_T$. The first two terms represent the left and right reservoirs in the noninteracting particle approximation, $H_\nu = \sum_{k\sigma} \varepsilon_{\nu k\sigma} c_{\nu k\sigma}^\dagger c_{\nu k\sigma}$, where $\varepsilon_{\nu k\sigma}$ denotes energy

of an electron with the wave number k and spin σ in the lead $\nu = L, R$. The dot Hamiltonian H_D involves two terms, $H_D = \sum_{\sigma=\uparrow,\downarrow} \varepsilon_\sigma d_\sigma^\dagger d_\sigma + U d_\uparrow^\dagger d_\uparrow d_\downarrow^\dagger d_\downarrow$, where the first term describes noninteracting electrons in the dot, whereas the second one takes into account Coulomb interaction with U denoting the correlation parameter. The tunneling Hamiltonian reads, $H_T = \sum_{\nu=L,R} \sum_{k\sigma} (T_\nu c_{\nu k\sigma}^\dagger d_\sigma + T_\nu^* d_\sigma^\dagger c_{\nu k\sigma})$, where T_ν denotes the corresponding tunnel matrix elements. Coupling of the dot to external leads can be described by the parameters $\Gamma_\nu^\sigma = 2\pi |T_\nu|^2 \rho_{\nu\sigma}$, with $\rho_{\nu\sigma}$ being the spin-dependent density of states in the lead ν . When defining the spin polarization of lead ν as $p_\nu = (\Gamma_\nu^+ - \Gamma_\nu^-)/(\Gamma_\nu^+ + \Gamma_\nu^-)$, the coupling parameters can be written as $\Gamma_\nu^{+(-)} = \Gamma_\nu(1 \pm p_\nu)$, with $\Gamma_\nu = (\Gamma_\nu^+ + \Gamma_\nu^-)/2$. Here, Γ_ν^+ and Γ_ν^- correspond to spin-majority and spin-minority electrons, respectively. In the following we assume $\Gamma_L = \Gamma_R \equiv \Gamma/2$. In the weak coupling regime, typical values of the dot-lead coupling strength Γ are of the order of tens of μeV , whereas the measurements are usually carried out at temperatures of the order of tens of mK^{31} .

In order to analyze electronic transport in the cotunneling regime we employ the second-order perturbation theory^{12,32}. The cotunneling rate for transition from the left to right leads is then given by

$$\gamma_{LR} = \frac{2\pi}{\hbar} \left| \sum_v \frac{\langle \Phi_L | H_T | \Phi_v \rangle \langle \Phi_v | H_T | \Phi_R \rangle}{\varepsilon_i - \varepsilon_v} \right|^2 \delta(\varepsilon_i - \varepsilon_f), \quad (1)$$

where ε_i and ε_f denote the energies of initial and final states, $|\Phi_\nu\rangle$ is the state with an electron in the lead ν , whereas $|\Phi_v\rangle$ is a virtual state with ε_v denoting the corresponding energy. Generally, one can distinguish between single-barrier and double-barrier cotunneling as well as between cotunneling processes that leave unchanged magnetic state of the dot and those which reverse spin of the dot. The non-spin-flip cotunneling processes are elastic and coherent, whereas the spin-flip ones are incoherent (and inelastic when the dot level is spin split). Unlike the double-barrier processes, the single-barrier ones do not contribute directly to electric current. However, they can change the occupation probabilities, and this way also the current flowing through the system.

In numerical calculations we have included all possible cotunneling events. Furthermore, we have allowed for intrinsic spin relaxation processes in the dot¹⁶. Such processes can result, for instance, from spin-orbit interaction in the dot or coupling of the electron spin to nuclear spins. We will not consider a particular microscopic mechanism of the intrinsic spin-flip processes, but simply assume their presence and describe them by the relevant spin-flip relaxation time τ_{sf} . The relaxation processes have been then taken into account *via* a relaxation term in the appropriate master equation for the occupation

probabilities,

$$0 = \sum_{\nu,\nu'=\text{L,R}} (-\gamma_{\nu\nu'}^{\sigma \rightarrow \bar{\sigma}} P_\sigma + \gamma_{\nu\nu'}^{\bar{\sigma} \rightarrow \sigma} P_{\bar{\sigma}}) - \frac{2}{\tau_{sf}} \frac{P_\sigma e^{\beta \varepsilon_\sigma} - P_{\bar{\sigma}} e^{\beta \varepsilon_{\bar{\sigma}}}}{e^{\beta \varepsilon_\sigma} + e^{\beta \varepsilon_{\bar{\sigma}}}}, \quad (2)$$

where $\beta = 1/(k_B T)$, P_σ denotes the probability that the dot is occupied by a spin- σ electron, and $\gamma_{\nu\nu'}^{\sigma \rightarrow \bar{\sigma}}$ is the cotunneling rate from lead ν to lead ν' with a change of the dot spin from σ to $\bar{\sigma}$ ($\bar{\sigma} = -\sigma$). The last term describes the spin relaxation processes. In the case of spin-degenerate dot level it is reduced to $-(P_\sigma - P_{\bar{\sigma}})/\tau_{sf}$. In the following we will distinguish between fast and slow spin relaxation limits. The fast (slow) spin relaxation corresponds to the case when the time between successive cotunneling events is significantly longer (shorter) than the intrinsic spin relaxation time τ_{sf} . The typical spin relaxation time for quantum dots can be relatively long, up to $\mu\text{s}^{33,34}$. On the other hand, when assuming typical parameters³¹, one can roughly estimate the time between two successive cotunneling events to range from 10^{-3} ns to 1 ns. Both the time between successive cotunneling events and the spin relaxation time depend on the system parameters and can be tuned, for example by applying a weak magnetic field, varying coupling to nuclear spins, etc. Thus, the regimes of fast and slow spin relaxation are achievable experimentally.

We consider the case when the dot is singly occupied at equilibrium and the system is in a deep Coulomb blockade regime; $\Gamma, k_B T \ll |\varepsilon_\sigma|, \varepsilon_\sigma + U$. In such a case the sequential tunneling is exponentially suppressed, and cotunneling gives the dominant contribution to electric current²⁰. Both non-spin-flip and spin-flip cotunneling processes are then allowed and have to be taken into account. The current flowing through the system from the left to right leads is given by

$$I = e \sum_{\sigma\sigma'} P_\sigma \left[\gamma_{LR}^{\sigma \rightarrow \sigma'} - \gamma_{RL}^{\sigma \rightarrow \sigma'} \right]. \quad (3)$$

In the following we discuss the influence of intrinsic spin relaxation on differential conductance and tunnel magnetoresistance of the quantum dot in the cotunneling regime both in the presence and absence of external magnetic field B . The TMR effect is defined as

$$\text{TMR} = \frac{I_P - I_{AP}}{I_{AP}}, \quad (4)$$

with I_P (I_{AP}) denoting the current flowing through the system in the parallel (antiparallel) magnetic configuration at a constant bias voltage V .

III. QUANTUM DOTS SYMMETRICALLY COUPLED TO THE LEADS

First, let us proceed with the case of quantum dots coupled to ferromagnetic leads with equal spin polarizations ($p_L = p_R \equiv p$). Our considerations will also include

the cases of quantum dots with non-degenerate and degenerate energy levels. The former situation is discussed in the following subsection.

A. The case of spin-degenerate dot level

In the case of $B = 0$ the dot level is spin degenerate, $\varepsilon_{\uparrow} = \varepsilon_{\downarrow} = \varepsilon$. The differential conductance $G = dI/dV$ for parallel and antiparallel magnetic configurations is shown in Fig. 1(a) for the case of no intrinsic spin relaxation in the dot ($1/\tau_{sf} \rightarrow 0$). In the parallel configuration one finds typical parabolic behavior of the conductance with increasing transport voltage. However, this is not the case for antiparallel configuration, where a maximum in the differential conductance appears in the small bias voltage regime. This anomalous behavior of the differential conductance, in turn, leads to respective minimum in the tunnel magnetoresistance, as shown by the solid curve in Fig. 1(c).

Physical mechanism of the zero-bias anomaly was considered in Ref. [20] for the case of no intrinsic spin relaxation. It was pointed out that the anomaly results from the relative difference between the fastest cotunneling events (which involve only the majority electrons of the leads) contributing directly to the charge current in the parallel and antiparallel configurations. In the parallel configuration, the main contribution to electric current comes from the non-spin-flip cotunneling processes, whereas spin-flip cotunneling is dominant for antiparallel alignment. In addition, the spin asymmetry in tunneling processes leads to a nonequilibrium spin accumulation in the dot in the antiparallel configuration, which increases with increasing bias voltage. The spin accumulation, defined as $(P_{\uparrow} - P_{\downarrow})/2$, is shown in Fig. 2 as a function of the bias voltage for different spin relaxation times. For the parameters assumed here and for negative bias ($eV < 0$, current flows from right to left, while electrons flow from left to right), there is a larger probability to find in the dot a spin-up electron than a spin-down one. This, in turn, diminishes the contribution coming from the fastest spin-flip cotunneling processes. However, there are also single-barrier spin-flip cotunneling events which reverse spin of the dot and open the system for the fastest transport processes. The rate of single-barrier processes is proportional to temperature (but independent of the applied voltage), whereas that of double-barrier processes increases with the transport voltage, being roughly independent of temperature. Thus, when $|eV| \lesssim k_B T$, the single-barrier processes play a significant role – they decrease the spin accumulation in the dot and open the system for the fastest cotunneling events. Consequently, the main contribution to current comes then from the most probable spin-flip cotunneling processes. When $|eV| \gg k_B T$, the relative role of single-barrier processes is diminished due to an increased role of double-barrier cotunneling, and the differential conductance decreases. The zero-bias maximum in differential conductance ap-

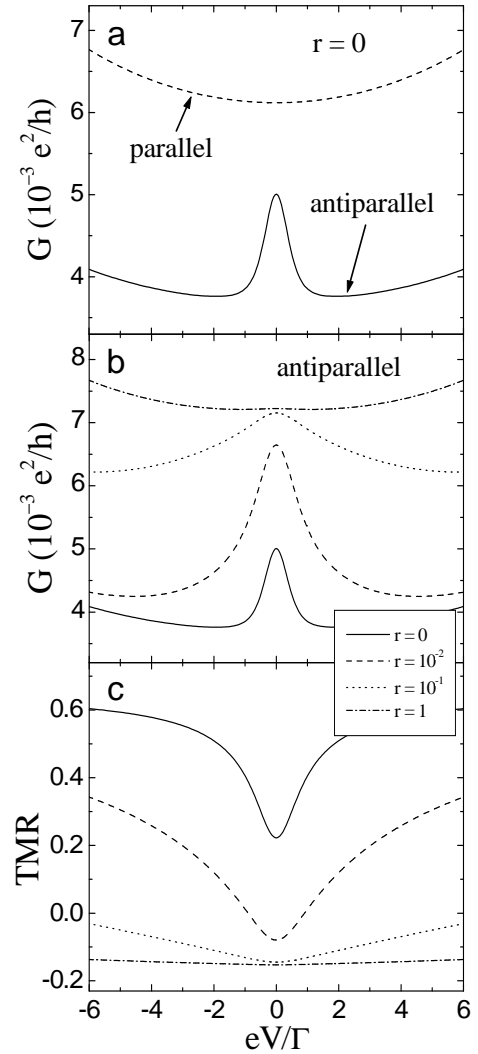


FIG. 1: The differential conductance in the parallel and antiparallel configurations (a,b) and tunnel magnetoresistance (c) as a function of the bias voltage for different spin relaxation $r = h/(\tau_{sf}\Gamma)$. The parameters are: $k_B T = 0.2\Gamma$, $\varepsilon = -15\Gamma$, $U = 30\Gamma$, and $p_L = p_R = 0.5$.

pears then as a result of the competition between single- and double-barrier cotunneling processes.

The anomalous behavior of differential conductance in the antiparallel configuration results from spin asymmetry of tunneling processes. This asymmetry leads to nonequivalent occupation of the dot by spin-up and spin-down electrons (spin accumulation), as illustrated in Fig. 2. From the above discussion follows that the spin accumulation is crucial for the occurrence of the zero-bias anomaly. Thus, one may expect that intrinsic spin-flip processes in the dot should suppress the anomaly. Indeed, intrinsic spin relaxation in the dot significantly modifies the conductance maximum at zero bias, and totally suppresses this anomalous behavior in the limit of fast spin relaxation. This behavior is displayed in Fig. 1(b), where different curves correspond to different

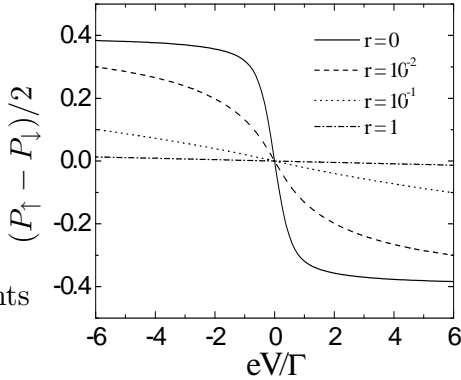


FIG. 2: The spin accumulation in the antiparallel configuration as a function of the bias voltage for different spin relaxation $r = h/(\tau_{sf}\Gamma)$. The parameters are the same as in Fig. 1.

values of the parameter r defined as $r = h/(\tau_{sf}\Gamma)$. Thus, $r = 0$ describes the case with no intrinsic spin relaxation, whereas the curves corresponding to nonzero r describe the influence of intrinsic relaxation processes. First of all, one can note that small amount of intrinsic spin-flip processes enhances the zero-bias anomaly [see the curve for $r = 10^{-2}$ in Fig. 1(b)]. This is because such processes play then a role similar to that of single-barrier spin-flip cotunneling. In the case of fast spin relaxation, on the other hand, the spin accumulation is suppressed and the anomaly disappears, as can be seen in Fig. 1(b) and Fig. 2 for $r = 1$. It is also worth noting that spin-flip processes in the dot enhance the overall conductance in the antiparallel configuration. In the parallel configuration, however, the differential conductance does not depend on intrinsic relaxation. This is because there is no spin accumulation in the parallel configuration, and consequently the intrinsic spin-flip processes in the dot do not play any role.

In the case of a deep Coulomb blockade one can take only the lowest order corrections in x/y , with $x = k_B T, |eV|$ and $y = |\varepsilon|, \varepsilon + U$, and derive some approximate formulas for the differential conductance. For the parallel configuration, the differential conductance can be then expressed as

$$G^P = \frac{e^2 \Gamma^2}{h} \left[\frac{1}{\varepsilon^2} + \frac{1}{(\varepsilon + U)^2} + \frac{1 - p^2}{|\varepsilon|(\varepsilon + U)} \right]. \quad (5)$$

In the antiparallel configuration and for $|eV| \ll k_B T$, the conductance is given by the expression

$$G_{\max}^{\text{AP}} = \frac{e^2 \Gamma^2}{h} \left\{ (1 - p^2) \left[\frac{1}{\varepsilon^2} + \frac{1}{(\varepsilon + U)^2} + \frac{1}{|\varepsilon|(\varepsilon + U)} \right] + \frac{p^2 U^2 h / \tau_{sf}}{\varepsilon^2 (\varepsilon + U)^2 h / \tau_{sf} + k_B T U^2 \Gamma^2} \right\}, \quad (6)$$

which describes the maximum of the differential conductance at zero bias for arbitrary value of r . On the other

hand, when $|eV| \gg k_B T$ and $r \ll 1$ one finds the formula

$$G_{\min}^{\text{AP}} = \frac{e^2 \Gamma^2}{h} \frac{1}{2} \left\{ \frac{1 - p^2}{1 + p^2} \left[\frac{1}{\varepsilon^2} + \frac{1}{(\varepsilon + U)^2} + \frac{1 - p^2}{|\varepsilon|(\varepsilon + U)} \right] + \frac{4p^2}{1 + p^2} \frac{U^2 h / \tau_{sf}}{2\varepsilon^2 (\varepsilon + U)^2 h / \tau_{sf} + (1 + p^2) k_B T U^2 \Gamma^2} \right\}, \quad (7)$$

which in turn approximates the local minimum value of the differential conductance. The expression for G_{\min}^{AP} for arbitrary spin relaxation time is too complex to be presented here. It is clearly evident from the above expressions that the conductance depends on intrinsic spin relaxation only in the antiparallel configuration, in agreement with numerical results. The variation of the linear conductance in the antiparallel configuration with the parameter r is displayed in Fig. 3(a) for several values of temperature. As one can see, there is a clear crossover between the limits of fast and slow spin relaxation in the dot. The crossover depends on temperature and is shifted towards shorter relaxation times as the temperature increases.

In order to describe the zero-bias anomaly in the differential conductance in the antiparallel configuration, it is useful to introduce the relative height of the maximum at $V = 0$, defined as $x_G = (G_{\max}^{\text{AP}} - G_{\min}^{\text{AP}})/G_{\min}^{\text{AP}}$. The variation of x_G with spin relaxation time is shown in Fig. 3(b) for different temperatures. First of all, one can see that the relative height depends on r in a nonmonotonic way. In the limit of slow spin relaxation and low temperature one finds $x_G = 4p^2/(3 - p^2)$, whereas in the limit of fast spin relaxation x_G tends to zero, independently of temperature, which can be also deduced from simple analysis of Eqs 6 and 7. Indeed, in the limit of fast spin relaxation G_{\max}^{AP} and G_{\min}^{AP} are equal and given by

$$G^{\text{AP}} = \frac{e^2 \Gamma^2}{h} \left[\frac{1}{\varepsilon^2} + \frac{1}{(\varepsilon + U)^2} + \frac{1 + p^2}{|\varepsilon|(\varepsilon + U)} \right]. \quad (8)$$

On the other hand, the relative height exhibits a maximum for a certain value of spin relaxation. This maximum, in turn, is decreased and shifts towards shorter relaxation times with increasing temperature, see Fig. 3(b). One can show that the maximum occurs when the relaxation time is approximately given by

$$\tau_{sf}^{\max} \approx \frac{h \varepsilon^2 (\varepsilon + U)^2}{k_B T U^2 \Gamma^2}. \quad (9)$$

The enhancement can range from a few percent for small spin polarization of the leads, $p \lesssim 0.2$, to several hundred percent for $p \gtrsim 0.9$. For the parameters assumed in Fig. 3(b), the zero-bias maximum in differential conductance for $\tau_{sf} = \tau_{sf}^{\max}$ is enhanced by about 65% as compared to the case of $\tau_{sf} \rightarrow \infty$. Assuming typical parameters for the quantum dot³¹, one can estimate τ_{sf}^{\max} as $\tau_{sf}^{\max} \approx 50\text{ns}$, which is accessible experimentally.^{33,34}

Intrinsic spin-flip scattering in the dot modifies conductance in the antiparallel configuration, and thus also the tunnel magnetoresistance, as shown in Fig. 1(c).

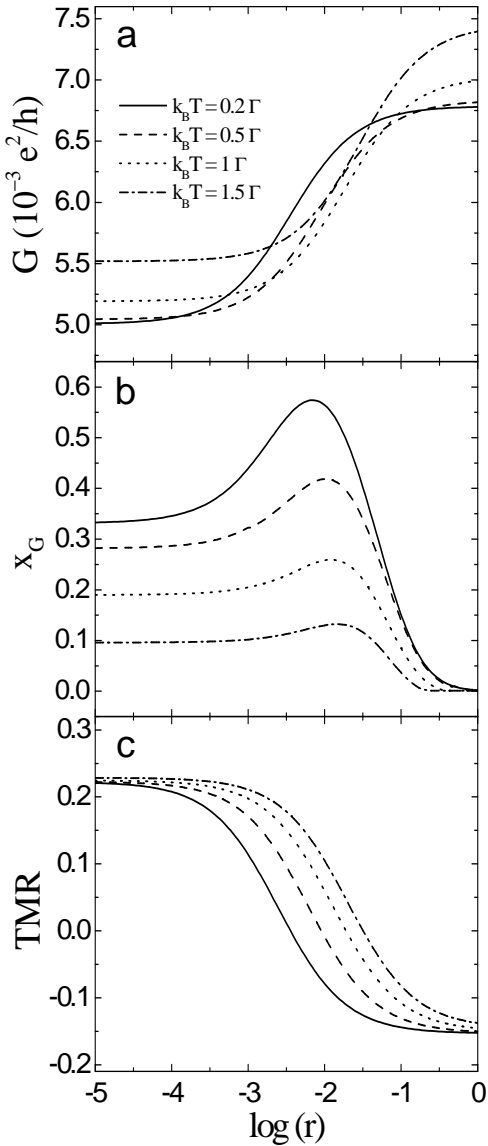


FIG. 3: The spin relaxation time dependence of the linear conductance in the antiparallel configuration (a) and the relative height of the zero-bias anomaly in differential conductance (b), as well as the linear-response TMR (c). The parameters are the same as in Fig. 1.

Since the zero-bias maximum in conductance is suppressed in the fast spin relaxation limit, the corresponding dip in TMR at small voltages is also suppressed by the intrinsic relaxation processes. More specifically, the dip in TMR broadens with increasing r and disappears in the limit of fast relaxation (see the curve for $r = 1$).

An interesting and new feature of TMR in the presence of spin-flip scattering in the dot is the crossover from positive to negative values when r increases, as illustrated in Fig. 1(c). Thus, the difference between conductances in the parallel and antiparallel magnetic configurations persists even for fast spin relaxation in the dot, contrary to the sequential tunneling regime, where

such a difference disappears¹⁶. This seemingly counter-intuitive behavior can be understood by taking into account the following two facts: (i) absence of spin accumulation in the dot for fast spin relaxation ($P_\uparrow = P_\downarrow$), and (ii) difference in the fastest cotunneling processes contributing to the current in the two magnetic configurations. As the point (i) is rather obvious in view of the results presented in Fig. 2, the point (ii) requires some additional clarification. The fastest double-barrier cotunneling processes involve only the majority-spin electrons of the two leads, thus, in the parallel configuration the fastest cotunneling processes are the non-spin-flip ones. They take place either *via* the empty-dot virtual state (for one orientation of the dot spin) or *via* the doubly occupied dot virtual state (for the second orientation of the dot spin). The dominant contribution to the current is then proportional to $1/\varepsilon^2 + 1/(\varepsilon + U)^2$. On the other hand, in the antiparallel magnetic configuration the fastest cotunneling processes are the spin-flip ones, which can occur only for one particular orientation of the dot spin. However, for this spin orientation cotunneling can take place *via* both empty and doubly occupied dot virtual states. The corresponding dominant contribution to electric current is then proportional to $[1/\varepsilon - 1/(\varepsilon + U)]^2 = 1/\varepsilon^2 + 1/(\varepsilon + U)^2 - 2/[\varepsilon(\varepsilon + U)]$. It is thus clear that the difference in currents flowing through the system in the antiparallel and parallel configurations is equal to $-2/[\varepsilon(\varepsilon + U)]$, which results from the interference term. Since $\varepsilon < 0$ and $\varepsilon + U > 0$, this interference contribution is positive. As a consequence, the current in the antiparallel configuration is larger than the current in the parallel configuration.

An analysis similar to that done above for differential conductance [see Eqs (5)-(7)] can be performed for tunnel magnetoresistance. The minimum in TMR at zero bias in the case of a symmetric Anderson model can be then expressed as

$$TMR_{\min} = \frac{2p^2 (4k_B T \Gamma^2 - \varepsilon^2 h / \tau_{sf})}{12(1 - p^2)k_B T \Gamma^2 + (3 + p^2)\varepsilon^2 h / \tau_{sf}}, \quad (10)$$

whereas for $|eV| \gg k_B T$ and $r \ll 1$ one finds

$$TMR_{\max} = \frac{2p^2 [2(3 - p^2)k_B T \Gamma^2 - \varepsilon^2 h / \tau_{sf}]}{2(1 - p^2)(3 - p^2)k_B T \Gamma^2 + (3 + p^2)\varepsilon^2 h / \tau_{sf}}. \quad (11)$$

The latter formula approximates the value of TMR corresponding to the bias voltage at which the differential conductance has a local minimum. In the slow spin relaxation limit one finds $TMR_{\min} = 2p^2/(3 - 3p^2)$, and $TMR_{\max} = 2p^2/(1 - p^2)$. However, in the limit of fast spin relaxation TMR becomes negative and is given by

$$TMR_{\min} = TMR_{\max} = -2p^2/(3 + p^2), \quad (12)$$

which is consistent with numerical results displayed in Fig. 1(c).

The explicit variation of the minimum in TMR at zero bias with spin relaxation time is shown in Fig. 3(c). The

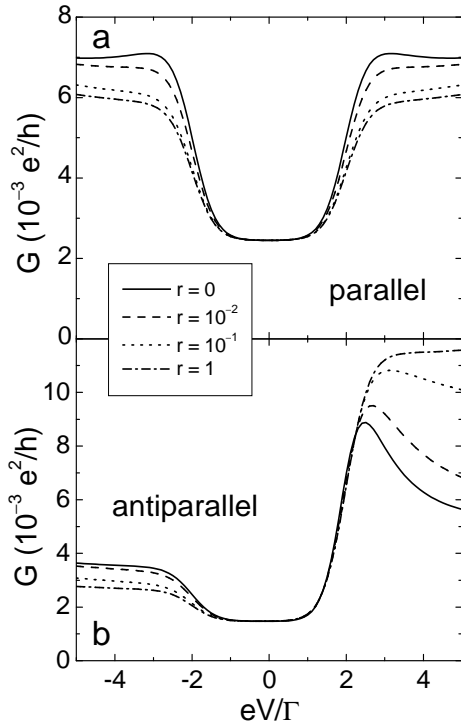


FIG. 4: The differential conductance in the nonlinear response regime for different spin relaxation in the parallel (a) and antiparallel (b) configurations. The parameters are: $k_B T = 0.2\Gamma$, $\varepsilon_\uparrow = -16\Gamma$, $\varepsilon_\downarrow = -14\Gamma$, $U = 30\Gamma$ and $p = 0.5$.

transition between slow and fast spin relaxation in the dot is clearly evident. This transition is associated with a change of the TMR sign from positive to negative. The crossover depends on temperature in a way similar to that found for the linear conductance and relative height of the zero-bias anomaly.

B. The case of spin-split dot level

The discussion up to now was limited to the case of a degenerate dot level. The situation changes when $\varepsilon_\uparrow \neq \varepsilon_\downarrow$, e.g., due to an external magnetic field. The magnetic field splits the dot level, consequently the occupation probabilities for the spin-up and spin-down electrons are not equal at equilibrium ($V = 0$). The level splitting is described by the parameter $\Delta = \varepsilon_\downarrow - \varepsilon_\uparrow$, where the magnetic field is assumed to be along the magnetic moment of the left electrode. In Fig. 4 we show the bias dependence of the differential conductance in the parallel and antiparallel configurations for different values of parameter r . In the limit of no intrinsic spin relaxation in the dot (solid line in Fig. 4) and at low bias voltage, the dot is occupied by a spin-up electron and the current flows mainly due to non-spin-flip cotunneling. The spin-flip cotunneling processes are suppressed for $|\Delta| \geq |eV|, k_B T$, which results in the steps in differential conductance at $|\Delta| \simeq |eV|$. The suppression

of spin-flip inelastic cotunneling was recently used as a tool to determine the spectroscopic g -factor³¹. When $|eV|$ becomes larger than $|\Delta|$, spin-flip cotunneling is allowed, consequently the conductance increases. However, there is a large asymmetry in the antiparallel configuration with respect to the bias reversal. To understand this asymmetry, it is crucial to realize that when the splitting $\Delta = \varepsilon_\downarrow - \varepsilon_\uparrow$ is larger than $k_B T$, the single-barrier spin-flip cotunneling processes can occur only when the dot is occupied by a spin-down electron. This follows simply from the energy conservation rule. (The situation may be changed for negative Δ .) Thus, the single-barrier processes can assist the fastest double-barrier cotunneling processes, but only for positive bias. This is because the fastest processes can occur when the dot is occupied by a spin-down electron for negative bias and by a spin-up electron for positive bias, leading to larger conductance for positive than for negative bias voltage. This is indeed the case in the numerically calculated characteristics shown in Fig. 4(b). No such asymmetry occurs in the parallel configuration [see Fig. 4(a)], as now the system is fully symmetric with respect to bias reversal.

The situation changes when intrinsic spin-flip relaxation processes occur in the dot. For the parameters assumed in Fig. 4, the spin relaxation in the dot affects the conductance only for $|eV| \gtrsim |\Delta|$, while for $|eV| \lesssim |\Delta|$ the conductance is basically independent of r (see Fig. 4). This is because for $|eV| \lesssim |\Delta|$ and $|\Delta| \gg k_B T$, the dot is predominantly occupied by a spin-up electron and the transitions to the spin-down state due to relaxation processes are energetically forbidden. As a consequence, the current flows mainly due to non-spin-flip cotunneling, irrespective of spin relaxation time. This scenario holds for both magnetic configurations of the system.

When $|eV| \gtrsim |\Delta|$, the spin-flip cotunneling processes can take place and the dot can be either in the spin-up or spin-down state. In the parallel configuration, Fig. 4(a), the conductance is slightly reduced by the spin-flip relaxation processes. This can be understood by realizing that the fastest non-spin-flip cotunneling processes in the parallel configuration are more probable when the dot is occupied by a spin-down electron than by a spin-up one (due to a smaller energy denominator, see Eq. 1). Since the spin-down state (as that of larger energy) relaxes relatively fast to the spin-up state (which has definitely smaller energy), this leads to a reduction in the conductance. On the other hand, the differential conductance in the antiparallel configuration is enhanced by the relaxation processes for positive bias and diminished for negative bias voltages. Consider first the situation for positive bias. As already discussed above for $r = 0$, an important role in that transport regime is played by the single-barrier spin-flip cotunneling processes, which open the system for the fast double-barrier cotunneling by reversing spin of the dot from the spin-down to the spin-up state. The relaxation processes play a role similar to that of the single-barrier cotunneling, and lead to a certain increase in the conductance. For negative

bias voltage, in turn, the fast double-barrier cotunneling processes occur when the dot is occupied by a spin-down electron. Probability of this is reduced by the spin relaxation processes, which leads to a reduced conductance. An interesting consequence of the enhancement (reduction) of the conductance for positive (negative) bias voltage is an increase of the asymmetry with respect to the bias reversal – see the curve for $r = 1$ in Fig. 4(b).

IV. QUANTUM DOTS ASYMMETRICALLY COUPLED TO THE LEADS

An interesting situation occurs when the quantum dot is coupled asymmetrically to the left and right leads ($p_L \neq p_R$). For this situation we first present the results in the case of degenerate dot level and then proceed with the discussion of the case when the degeneracy is lifted, e.g. by an external magnetic field.

A. The case of spin-degenerate dot level

The differential conductance for a system with one electrode nonmagnetic and the other one made of a ferromagnet with large spin polarization (in the following referred to as strong ferromagnet) is shown in Fig. 5. The parts (a) and (c) correspond to the cases when the dot is described by an asymmetric Anderson model ($|\varepsilon| \neq \varepsilon + U$). The difference between (a) and (c) is due to different position of the dot level ε , and consequently also $\varepsilon + U$, with respect to the Fermi level at equilibrium. More precisely, (a) and (c) are symmetric in the sense that $|\varepsilon|$ in (a) is equal to $\varepsilon + U$ in (c), and vice-versa, $|\varepsilon|$ in (c) is equal to $\varepsilon + U$ in (a). Part (b), in turn, corresponds to the dot described by a symmetric Anderson model, with $|\varepsilon|$ equal to $\varepsilon + U$.

Consider first the situation in the absence of intrinsic spin relaxation in the dot (solid curves in Fig. 5). There is then a significant asymmetry of electric current with respect to the bias reversal in the situations displayed in Fig. 5(a) and (c), whereas no such an asymmetry occurs for the symmetric Anderson model [part (b)]. Another feature of the curves shown in Fig. 5 is the presence of zero-bias anomaly in the case described by the symmetric Anderson model [part (b)]. This anomaly is similar to that shown in Fig. 1(a) for antiparallel configuration. The anomaly still exists, although it is less pronounced when the dot is described by the asymmetric Anderson model, as clearly visible in Fig. 5(a) and (c).

Let us discuss now the physical mechanism of the asymmetry with respect to the bias reversal displayed in Fig. 5(a) and (c). When $|eV| \gg k_B T$, one can neglect the influence of single-barrier cotunneling²⁰. The cotunneling processes which transfer charge from one lead to another take place *via* two possible virtual states – empty dot (an electron residing in the dot tunnels to one of the leads and another electron from the second lead enters

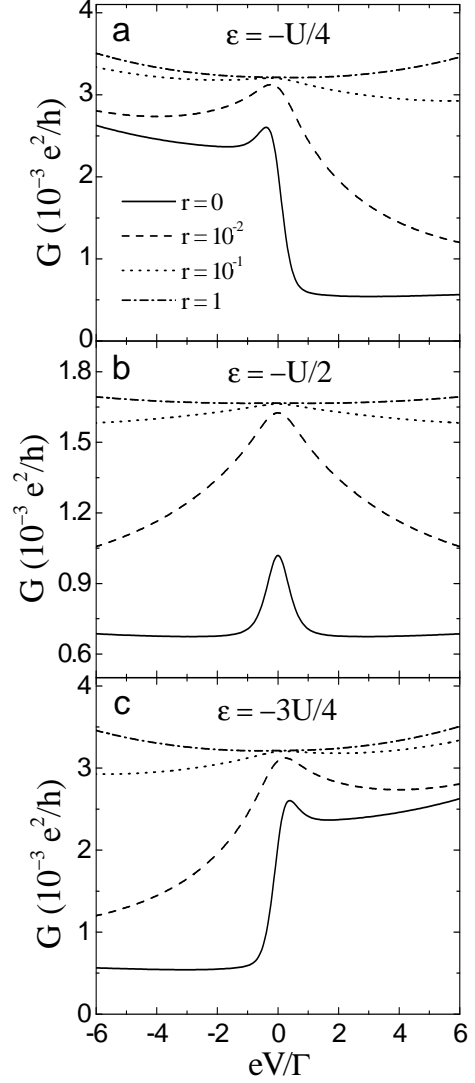


FIG. 5: The differential conductance in the nonlinear response regime for the asymmetric (a,c) and symmetric (b) Anderson model for different spin relaxation. The parameters are: $k_B T = 0.2\Gamma$, $U = 60\Gamma$, $p_L = 0.95$ and $p_R = 0$.

the dot) and doubly occupied dot (an electron of spin opposite to that in the dot enters the dot and then one of the two electrons leaves the dot). Consider first the situation shown in Fig. 5(a) for positive bias ($eV > 0$, electrons flow from right to left, i.e., from normal metal to strong ferromagnet), and assume for clarity of discussion that the strong ferromagnet is a half-metallic one with full spin polarization (only spin-up electrons can then tunnel to the left lead). When a spin-down electron enters the dot, it has no possibility to leave the dot for a long time. The allowed cotunneling processes occur then *via* doubly occupied dot virtual states. In the absence of intrinsic spin relaxation in the dot, the only processes which can reverse the dot spin are the single-barrier cotunneling ones, which however play a minor role when $k_B T \ll |eV|$. Thus, the current flows due to non-spin-flip cotunneling

via doubly-occupied dot virtual states, whereas cotunneling through empty-dot virtual states is suppressed. The situation is changed for negative bias (electrons flow from strong ferromagnet to normal metal). Now, the dot is mostly occupied by a spin-up electron, which suppresses cotunneling *via* doubly-occupied dot virtual state and the only contribution comes from cotunneling *via* empty-dot virtual state. The ratio of cotunneling rates through the empty dot and doubly occupied dot virtual states is approximately equal to $\xi = [\varepsilon/(\varepsilon + U)]^{-2}$. In the situation presented in Fig. 5(a) one finds $\xi \gg 1$. Accordingly, the conductance for negative bias is much larger than for positive bias voltage. In turn, in the case displayed in Fig. 5(c) the ratio of the respective cotunneling rates is exactly equal to the inverse of this ratio corresponding to the case shown in Fig. 5(a). Thus, now we have $\xi \ll 1$, and the conductance is smaller for negative bias than for positive. In turn, in the case presented in Fig. 5(b) the ratio ξ is equal to 1, consequently both cotunneling rates are equal and the conductance is symmetric with respect to the bias reversal.

When $|eV|$ becomes of the order of $k_B T$ or smaller, the rate of single-barrier cotunneling is of the order of the rate of double-barrier cotunneling. Therefore, the single-barrier processes can play an important role in transport. More precisely, single-barrier cotunneling processes can reverse spin of an electron in the dot and thus can open the system for the fast cotunneling processes. This behavior can be observed in Fig. 5(a) and (c). In the symmetric case shown in Fig. 5(b), the single-barrier processes lead to the zero-bias anomaly similar to that shown in Fig. 1(a) for antiparallel configuration in a system with two ferromagnetic electrodes coupled symmetrically to the dot. The mechanism of the anomaly is the same, i.e., the single-barrier cotunneling, which occurs for $k_B T \gg |eV|$, opens the system for the fast cotunneling processes. This leads to an increase in conductance in the small bias range. The zero-bias anomaly exists also in asymmetric cases illustrated in Fig. 5(a) and (c). However, the maximum in conductance is slightly shifted away from $V = 0$ and is much less pronounced.

Intrinsic spin-flip processes in the dot have similar influence on electronic transport as in the symmetric case studied in the previous section. As before, relaxation processes remove the asymmetry with respect to the bias reversal and suppress the zero-bias anomaly. Thus, the diode-like behavior can appear only in the limit of slow spin relaxation, and is suppressed in the limit of fast spin relaxation, as shown in Fig. 5 by the curves corresponding to $r = 1$.

Some analytical expressions for the conductance can be obtained in the limit $|eV| \gg k_B T$ and when assuming $p_L = p$, $p_R = 0$. The approximate formulas for the

differential conductance then read

$$G = \frac{e^2 \Gamma^2}{h} \left[\frac{1}{(\varepsilon + U)^2} + \frac{(1 - p^2)U}{\varepsilon^2(\varepsilon + U)} \right. \\ \left. + \frac{p^2 \varepsilon^2 U (\varepsilon + U)^3}{[\varepsilon^2(\varepsilon + U)^2 - eVU^2 \Gamma^2 \tau_{sf} / (4h)]^2} \right] \quad (13)$$

for positive bias, and

$$G = \frac{e^2 \Gamma^2}{h} \left[\frac{1}{\varepsilon^2} + \frac{(1 - p^2)U}{|\varepsilon|(\varepsilon + U)^2} \right. \\ \left. + \frac{p^2 |\varepsilon|^3 U (\varepsilon + U)^2}{[\varepsilon^2(\varepsilon + U)^2 + eVU^2 \Gamma^2 \tau_{sf} / (4h)]^2} \right] \quad (14)$$

for negative bias. In order to describe the diode operation it is useful to define the ratio α of the conductances for positive and negative bias voltages. In the limit of long spin relaxation the ratio α is given by

$$\alpha = \frac{\varepsilon^2 + (1 - p^2)(\varepsilon + U)U}{(\varepsilon + U)^2 + (1 - p^2)|\varepsilon|U}. \quad (15)$$

It is worth noting that the operation of the diode can be tuned by the gate voltage (which shifts energy of the dot level).

B. The case of spin-split dot level

In Figure 6 we illustrate the influence of spin splitting of the dot level due to an applied magnetic field, $\varepsilon_\uparrow \neq \varepsilon_\downarrow$. The bias voltage dependence of the differential conductance is shown there for different values of the parameter r , for symmetric (b) and asymmetric (a,c) Anderson models. The parameters used in numerical calculations are the same as in Fig. 5, except for the dot level energy which was spin degenerate in Fig. 5 and now is spin split.

Let us first focus on Fig. 6(a), which corresponds to the case of asymmetric Anderson model, $\varepsilon = -U/4$. Two new features of the conductance in the limit of no intrinsic spin relaxation appear in this figure. First, the conductance is now suppressed above a certain finite positive value of the bias voltage, and not for $eV > 0$ as in the case shown in Fig. 5(a). Strictly speaking, the conductance drops when eV is equal to the level splitting Δ , $eV \approx \Delta$. The shift of the main slope in the conductance from $eV = 0$ to $eV \approx \Delta$ is due to the fact that the dot is blocked for cotunneling *via* the empty state by a spin-down electron only when eV exceeds the level splitting. This results from the energy conservation. Thus, in the case shown in Fig. 5(a) the main drop of the conductance was at $eV = 0$, whereas in Fig. 6(a) it is at $eV \approx \Delta$. When a spin-down electron appears in the dot, then, for $eV < \Delta$, it can always tunnel back to the source electrode and open the dot for fast cotunneling through the empty state.

The second feature of the differential conductance in the $r = 0$ case is the peak at $eV \approx \Delta$, and a shallow

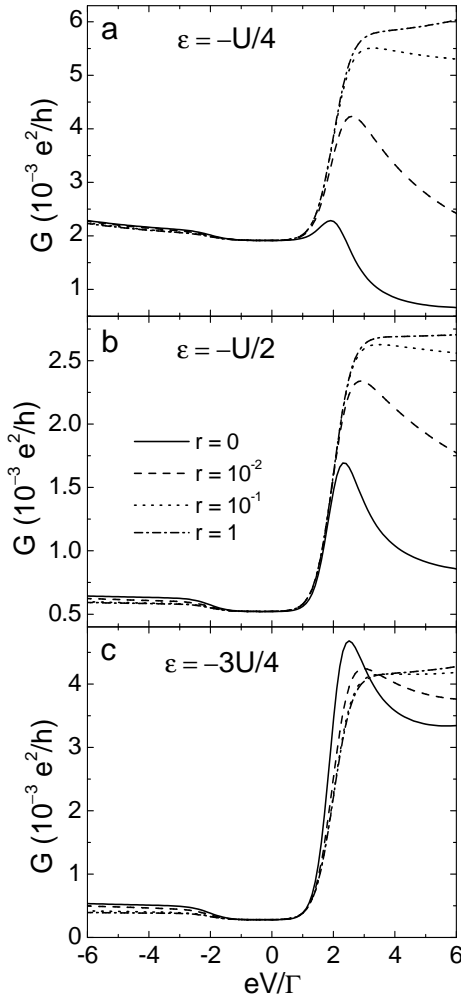


FIG. 6: The differential conductance in the nonlinear response regime for different spin relaxation. The parameters are: $k_B T = 0.2\Gamma$, $\varepsilon_\uparrow = \varepsilon - \Delta/2$, $\varepsilon_\downarrow = \varepsilon + \Delta/2$, $\Delta = 2\Gamma$, $U = 60\Gamma$, $p_L = 0.95$ and $p_R = 0$.

plateau for $|eV| \lesssim \Delta$. The origin of the peak is similar to the origin of the zero-bias anomaly in the case of spin-degenerate dot level. On the other hand, the plateau in the small bias range is due to suppression of the spin-flip cotunneling for $|eV| \lesssim \Delta$, similarly as in Fig. 4. However, the plateau is now very weak and shallow. This is a consequence of the minor role of the spin-flip cotunneling, which results from the strong spin polarization of ferromagnetic electrode.

Qualitatively similar behavior may be also observed for $\varepsilon = -3U/4$. This situation is shown in Fig. 6(c) and is analogous to the one illustrated in Fig. 5(c). In the case of $\varepsilon = -U/2$ shown in Fig. 6(b), the influence of magnetic field is qualitatively similar to that found in the case of

a quantum dot coupled to two ferromagnetic leads in the antiparallel configuration, see Fig. 4.

Transport characteristics are modified by the spin relaxation in the dot. As before, the changes occur for $|eV| \gtrsim |\Delta|$. For positive bias voltage, the spin relaxation processes modify the conductance mainly for $\varepsilon = -U/4$ and $\varepsilon = -U/2$ [Fig. 6(a,b)], while for $\varepsilon = -3U/4$ [Fig. 6(c)] the changes are significantly smaller. For negative bias, on the other hand, the conductance is slightly suppressed by the spin relaxation. This is because for negative bias the dot is mainly occupied by a spin-up electron, and spin relaxation from the spin-up to spin-down dot states is suppressed due to $\Delta \gg k_B T$. Contrarily, for positive bias, $|eV| \gtrsim |\Delta|$, and for $\tau_{sf} \rightarrow \infty$, the dot is mostly occupied by a spin-down electron. Spin relaxation processes in the dot lead then to a certain increase in the occupation probability of the spin-up dot level, $P_\uparrow \approx 1$ in the long spin relaxation time limit. This in turn may lead to an increase in the differential conductance.

V. CONCLUDING REMARKS

We have considered numerically and analytically the influence of intrinsic spin relaxation in the dot on the differential conductance and the TMR effect in the cotunneling regime. It has been shown that the zero-bias anomaly in the antiparallel configuration is enhanced in the weak spin-flip scattering regime in the dot. The optimal conditions for a maximum enhancement have also been derived. However, in the limit of fast spin relaxation both the zero-bias anomaly and the dip in tunnel magnetoresistance at zero bias become suppressed. Moreover, we have found the inversion of sign of tunnel magnetoresistance in the presence of fast intrinsic spin relaxation in the dot.

We have also demonstrated that the zero-bias anomaly exists in systems with only one ferromagnetic electrode (the second one may be nonmagnetic). Such devices display diode-like transport characteristics. The diode-like behavior exists also when the system is in an external magnetic field, but the operation range is changed, i.e., the bias at which the conductance drops depends on the level splitting (magnetic field). Furthermore, we have shown that this behavior may be enhanced by intrinsic spin relaxation processes in the dot.

The work was supported by the Polish State Committee for Scientific Research through the projects PBZ/KBN/044/P03/2001 and 2 P03B 116 25. We also acknowledge discussions with Jan Martinek and Jürgen König.

* Electronic address: weymann@amu.edu.pl

¹ J. Barnaś and A. Fert, Phys. Rev. Lett. **80**, 1058 (1998).

² I. Weymann and J. Barnaś, *Phys. Stat. Sol. (b)* **236**, 651 (2003).

³ F. Ernult, K. Yamane, S. Mitani, K. Yakushiji, K. Takanashi, Y. K. Takahashi, K. Hono, *Appl. Phys. Lett.* **84**, 3106 (2004).

⁴ H. Shimada and Y. Ootuka, *Phys. Rev. B* **64**, 235418 (2002).

⁵ K. Yakushiji, F. Ernult, H. Imamura, K. Yamane, S. Mitani, K. Takanashi, S. Takahashi, S. Maekawa, H. Fujimori, *Nature Materials* **4**, 57 (2005).

⁶ I. Weymann, J. Barnaś, *Phys. Rev. B* **73**, 033409 (2006).

⁷ L. P. Kouwenhoven, C. M. Marcus, P. L. McEuen, S. Tarucha, R. M. Westervelt, and N. S. Wingreen, in *Proceedings of the NATO Advanced Study Institute on Mesoscopic Electron Transport*, Eds. L. L. Sohn, L. P. Kouwenhoven, and G. Schön (Kluwer Series E345, 1997).

⁸ L. Kouwenhoven and C. Marcus, *Physics World*, June 1998, p.35.

⁹ M. M. Deshmukh and D. C. Ralph, *Phys. Rev. Lett.* **89**, 266803 (2002).

¹⁰ R. Hanson, B. Witkamp, L. M. K. Vandersypen, L. H. Willems van Beveren, J. M. Elzerman, and L. P. Kouwenhoven, *Phys. Rev. Lett.* **91**, 196802 (2003).

¹¹ D. M. Zumbuhl, C. M. Marcus, M. P. Hanson, and A. C. Gossard, *Phys. Rev. Lett.* **93**, 256801 (2004).

¹² D. V. Averin and Yu. V. Nazarov, *Phys. Rev. Lett.* **65**, 2446 (1990).

¹³ L. J. Geerligs, D. V. Averin, and J. E. Mooij, *Phys. Rev. Lett.* **65**, 3037 (1990).

¹⁴ V. N. Golovach and D. Loss, *Phys. Rev. B* **69**, 245327 (2004).

¹⁵ B. R. Bułka, *Phys. Rev. B* **62**, 1186 (2000).

¹⁶ W. Rudziński and J. Barnaś, *Phys. Rev. B* **64**, 085318 (2001).

¹⁷ J. König and J. Martinek, *Phys. Rev. Lett.* **90**, 166602 (2003).

¹⁸ M. Braun, J. König, J. Martinek, *Phys. Rev. B* **70**, 195345 (2004).

¹⁹ M. Braun, J. König, J. Martinek, cond-mat/0601366.

²⁰ I. Weymann, J. Barnaś, J. König, J. Martinek, and G. Schön, *Phys. Rev. B* **72**, 113301 (2005).

²¹ J. N. Pedersen, J. Q. Thomassen, and K. Flensberg, *Phys. Rev. B* **72**, 045341 (2005).

²² I. Weymann and J. Barnaś, *Eur. Phys. J. B* **46**, 289 (2005).

²³ I. Weymann, J. König, J. Martinek, J. Barnaś, and G. Schön, *Phys. Rev. B* **72**, 115334 (2005).

²⁴ Y. Chye, M. E. White, E. Johnston-Halperin, B. D. Gerardot, D. D. Awschalom, and P. M. Petroff, *Phys. Rev. B* **66**, 201301(R) (2002).

²⁵ M. M. Deshmukh and D. C. Ralph, *Phys. Rev. Lett.* **89**, 266803 (2002).

²⁶ L. Y. Zhang, C. Y. Wang, Y. G. Wei, X. Y. Liu, and D. Davidović, *Phys. Rev. B* **72**, 155445 (2005).

²⁷ K. Tsukagoshi, B. W. Alphenaar, and H. Ago, *Nature* **401**, 572 (1999).

²⁸ B. Zhao, I. Mönch, H. Vinzelberg, T. Mühl, and C. M. Schneider, *Appl. Phys. Lett.* **80**, 3144 (2002); *J. Appl. Phys.* **91**, 7026 (2002).

²⁹ S. Sahoo, T. Kontos, J. Furer, C. Hoffmann, M. Gräber, A. Cottet, and C. Schönenberger, *Nature Physics* **1**, 102 (2005).

³⁰ A. N. Pasupathy, R. C. Bialczak, J. Martinek, J. E. Grose, L. A. K. Donev, P. L. McEuen, and D. C. Ralph, *Science* **306**, 86 (2004).

³¹ A. Kogan, S. Amasha, D. Goldhaber-Gordon, G. Granger, M.A. Kastner, and H. Shtrikman, *Phys. Rev. Lett.* **93**, 166602 (2004).

³² K. Kang and B. I. Min, *Phys. Rev. B* **55**, 15412 (1997).

³³ T. Fujisawa, D. G. Austing, Y. Tokura, Y. Hirayama, and S. Tarucha, *Nature (London)* **419**, 278 (2002).

³⁴ J. M. Elzerman, R. Hanson, L. H. W. van Beveren, B. Witkamp, L. M. K. Vandersypen, and L. P. Kouwenhoven, *Nature (London)* **430**, 6998 (2004).